GALVANOMAGNETIC PHENOMENA IN ANTIMONY AT LOW TEMPERATURES

M. S. BRESLER and N. A. RED'KO

Institute of Semiconductors, USSR Academy of Sciences

Submitted January 21, 1971

Zh. Eksp. Teor. Fiz. **61**, 287–300 (July, 1971)

Analysis of the experimental data on the temperature dependence of the electrical resistance of antimony single crystals shows that three mechanisms play an essential role in the scattering of current carriers: scattering by impurities and defects, intravalley acoustic scattering, and intervalley scattering. The components of the magneto-resistance tensor are measured for single-crystal antimony samples oriented along the principal crystallographic axes at temperatures of 77, 20.4, 14.5 and 4.2°K. Electron and hole mobilities and their temperature dependences are determined on the basis of measurements of the magneto-resistance tensor components. The deformation potential constant for electrons is estimated to be equal to ~ 6 eV.

THEORETICAL calculations[1] and experimental data[2-7] permit us to explain in detail the energy spectrum of the current carriers in antimony. It has been established that the Fermi surface of antimony consists of three electron and six hole cavities which in many cases can be approximated with sufficient accuracy by ellipsoids located in the planes of reflection and rotated about the binary axis C_2 by an angle of 6° for electrons and about 30° for holes relative to the basis plane. The electron cavities of the Fermi surface are located at the points L of the Brillouin zone, and the hole cavities three near each point T.

Such a model of the energy spectrum has been used with success for the interpretation of the results of galvanomagnetic phenomena in weak magnetic fields in the region from nitrogen to room temperature in[8,9], where the components of the electron and hole mobility tensors have been completely determined and the temperature dependence of the mobilities in the given range of temperatures has been established.

The galvanomagnetic effects in antimony have been studied frequently also at liquid helium temperatures;[10-14] however, the analysis of the results in[11,12] has been carried out on the basis of the isotropic two-band model while the other researches have been devoted to the consideration of individual particular questions, for example, the temperature dependence of the anisotropy of the magnetoresistance in strong magnetic fields[13] or quantum phenomena in pulsed magnetic fields.[14]

The detailed study of classical galvanomagnetic effects at temperatures below nitrogen temperatures are lacking in the literature. Information on the temperature dependence of the components of the mobility of the electrons and holes below 77°K is also lacking.

In the present research, an investigation has been made of the magnetoconductivity tensor of antimony for nitrogen, hydrogen and helium temperatures in strong and intermediate magnetic fields, and an analysis of the experimental data has been carried out on the beam of formulas derived for the galvanomagnetic coefficients within the framework of the multiellipsoidal model.

1. THEORY

For the interpretation of the experimental results, we used the expressions for the electric conductivity tensor in a magnetic field. This tensor can be obtained within the framework of the multi-ellipsoidal model of the energy spectrum of electrons and holes. We shall assume that the electron and hole cavities of the Fermi surface of antimony can be approximated by ellipsoids, although they (in particular, the hole surfaces) generally have a more complicated shape.[1,6,7]

As usual, we shall introduce a set of coordinates with axes directed along the principal crystallographic directions (axis 1 along the binary axis, C_2, axis 2 along the bisector of the angle between the two binary axes, which lies in the plane of specular reflection and is perpendicular to the threefold axis C_3, while the axis 3 is directed along the axis C_3 of the crystal). The ellipsoids lie in reflection planes and are turned about the binary axis by the angle ϑ (ϑ_e for electrons, ϑ_h for holes) relative to the basis plane. The number of electron ellipsoids is equal to three, the number of hole ellipsoids to six, but since the hole ellipsoids pairwise make the same contribution to the electric current, we can tentatively assume that their number is three. We shall further assume (unless otherwise mentioned) that the electron concentration is equal to the hole concentration: $N = n = p$.

If we introduce phenomenologically the relaxation-time tensor, which is diagonal in the coordinate axes of the mass ellipsoid (this is correct for not too anisotropic scattering mechanisms[15,16] even with account of the anisotropy of the phonon spectrum[17]) then, solving the kinetic equation in a fashion similar to what was done in the work of Harman, Honig and Tarmy,[18] and taking it into account that for strong degeneracy of the gas of current carriers the averaging over the distribution function reduces to the substitution of $\tau(\epsilon_F)$ for $\tau(\epsilon)$, where ϵ_F is the Fermi energy, one can obtain an expression for the components of the electric conductivity tensor in a magnetic field. Such expressions for the components of the magnetoconductivity tensor are valid, however, only for elastic scattering mechanisms, and also in the case of not very

strong inelasticity, for example, in low-temperature acoustic scattering (which leads in the isotopic model of a metal with one type of carrier to the T^5 law for resistance). In the case of strong inelasticity (for example, for intervalley scattering), even if one introduces the relaxation time, it turns out to depend strongly on the energy near the Fermi energy ϵ_F, and the averaging over the distribution function cannot be reduced to the substitution $\tau(\epsilon) \to \tau(\epsilon_F)$.[19] Here, in the expressions for the components of the magnetoconductivity in terms of the mobilities, coefficients of the order of unity should appear, similar to the case of a nondegenerate gas. As is discussed further in the experimental part of the present paper, intervalley scattering can play a significant role in antimony even at liquid-nitrogen temperatures; therefore, the interpretation of the experimental data with the help of the cited formulas can lead to noticeable difference between calculation and experiment (of the order of several dozen percent).

Comparatively simple expressions for the components of the electric conductivity tensor in a magnetic field are obtained only in cases in which the magnetic field is oriented along the principal crystallographic directions. It is convenient to express the components of the electric conductivity tensor in terms of the components of the electron and hole mobility tensors $\hat{\mu}$ and $\hat{\nu}$, which are defined by

$$\hat{\mu} = e\hat{\tau}_e \hat{m}^{-1}, \quad \hat{\nu} = e\hat{\tau}_h \hat{m}_h^{-1}, \quad (1)$$

where e is the electron charge and $\hat{m}^{-1}$ is the reciprocal of the effective-mass tensor. For the "principal" ellipsoid, one axis of which coincides with the axis 1, and the other two are turned relative to the axes 2 and 3 by the angle ϑ, the tensor $\hat{\mu}$ has the form

$$\begin{vmatrix} \mu_1 & 0 & 0 \\ 0 & \mu_2 & \mu_4 \\ 0 & \mu_4 & \mu_3 \end{vmatrix}, \quad (2)$$

where $\mu_1 \equiv \mu_{11}$, $\mu_2 \equiv \mu_{22}$, $\mu_3 \equiv \mu_{33}$, $\mu_4 \equiv \mu_{23} = \mu_{32}$ in agreement with the usual notation; for the other two ellipsoids the tensor are obtained by rotation through $\pm 120°$ about axis 3.

We write down the results for the electric conductivity tensor in a magnetic field oriented in the principal crystallographic directions.

$$\sigma_{11} = e\frac{N}{3}\left[\mu_1 + \frac{1/2(\mu_1 + 3\mu_2) + 2\mu_1\varphi(\mu)H^2/c^2}{1 + 1/_4 f(\mu)H^2/c^2} + (\mu \to \nu) \right], \quad (3)$$

$$\sigma_{22} = e\frac{N}{3}\left[\frac{\mu_2}{1 + \varphi(\mu)H^2/c^2} + \frac{1/2(3\mu_1 + \mu_2)}{1 + 1/_4 f(\mu)H^2/c^2} + (\mu \to \nu) \right], \quad (4)$$

$$\sigma_{23} = e\frac{N}{3}\left[\frac{\mu_4 - \varphi(\mu)H/c}{1 + \varphi(\mu)H^2/c^2} - \frac{\mu_4 + 1/2 f(\mu)H/c}{1 + 1/_4 f(\mu)H^2/c^2} \right.$$
$$\left. + \frac{\nu_4 + \varphi(\nu)H/c}{1 + \varphi(\nu)H^2/c^2} - \frac{\nu_4 - 1/2 f(\nu)H/c}{1 + 1/_4 f(\nu)H^2/c^2} \right], \quad (5)$$

$$\sigma_{33} = e\frac{N}{3}\left[\frac{\mu_3}{1 + \varphi(\mu)H^2/c^2} + \frac{2\mu_3}{1 + 1/_4 f(\mu)H^2/c^2} + (\mu \to \nu) \right], \quad (6)$$
$$\sigma_{23}(H) = \sigma_{32}(-H).$$

(Here $f(\mu) = 3\mu_1\mu_3 + \mu_2\mu_3 - \mu_4^2$, $\varphi(\mu) = \mu_2\mu_3 - \mu_4^2$, and by $(\mu \to \nu)$ are meant terms obtained from the substitution $\mu \to \nu$.) The remaining components are equal to zero. We call attention to the components σ_{23} that are even in the magnetic field (in the following,

we denote these by σ_{23}^{II} in contrast with the odd ones σ_{23}^{I}), which is admitted by the symmetries of the antimony crystal and is connected with the inclination of the electron and hole ellipsoids relative to the axes of the crystal (the contributions to them are proportional to μ_4 and ν_4).

In strong magnetic fields the quantities

$$\varphi(\mu), 1/_4 f(\mu), \varphi(\nu), 1/_4 f(\nu) \gg c^2 H^{-2},$$
$$\sigma_{11} \sim H^0, \quad \sigma_{22} \sim H^{-2}, \quad \sigma_{23} \sim H^{-2}.$$

In the presence of a small difference in the concentration of holes and electrons, $\Delta N = p - n$, in sufficiently strong fields there is a significant contribution due to this increment (see[20] and the experimental data on bismuth in[21]), and the nondiagonal component σ_{23} has the form

$$\sigma_{23}^I = e\frac{\Delta Nc}{H} + e\frac{N}{3}\frac{c^3}{H^3}\left[\frac{1}{\varphi(\mu)} + \frac{8}{f(\mu)} - (\mu \to \nu) \right], \quad (7)$$

$$\sigma_{23}^{II} = e\frac{N}{3}\frac{c^2}{H^2}\left[\frac{\mu_4}{\varphi(\mu)} - \frac{4\mu_4}{f(\mu)} + (\mu \to \nu) \right]. \quad (8)$$

The transition from the components of the tensor $\hat{\rho}$ to the components of the tensor $\hat{\sigma}$ is found from the definition $\hat{\sigma}\hat{\rho} = 1$.

2) $H \parallel C_1 \parallel 2$. In this case, all the six independent components of the electric conductivity tensor in a magnetic field are different from zero:

$$\sigma_{11} = e\frac{N}{3}\left[\frac{\mu_1}{1 + \mu_1\mu_3 H^2/c^2} + \frac{1/2(\mu_1 + 3\mu_2)}{1 + 1/_4\psi(\mu)H^2/c^2} + (\mu \to \nu) \right], \quad (9)$$

$$\sigma_{12} = -\sigma_{21} = e\frac{N}{3}\frac{H}{c}\left[\frac{\mu_1\mu_4}{1 + 1/_4\psi(\mu)H^2/c^2} - \frac{\mu_1\mu_4}{1 + \mu_1\mu_3 H^2/c^2} - (\mu \to \nu) \right], \quad (10)$$

$$\sigma_{13} = -\sigma_{31} = e\frac{N}{3}\frac{H}{c}\left[-\frac{\mu_1\mu_3}{1 + \mu_1\mu_3 H^2/c^2} - \frac{1/2\psi(\mu)}{1 + 1/_4\psi(\mu)H^2/c^2} + (\mu \to \nu) \right], \quad (11)$$

$$\sigma_{22} = e\frac{N}{3}\left[\mu_2 - \frac{\mu_1\mu_4^2 H^2/c^2}{1 + \mu_1\mu_3 H^2/c^2} + \frac{1/2(3\mu_1 + \mu_2) + 2\mu_4\varphi(\mu)H^2/c^2}{1 + 1/_4\psi(\mu)H^2/c^2} \right.$$
$$\left. + (\mu \to \nu) \right], \quad (12)$$

$$\sigma_{23} = \sigma_{32} = e\frac{N}{3}\left[\frac{\mu_4}{1 + 1/_4\psi(\mu)H^2/c^2} - \frac{\mu_4}{1 + \mu_1\mu_3 H^2/c^2} - (\mu \to \nu) \right], \quad (13)$$

$$\sigma_{33} = e\frac{N}{3}\left[\frac{\mu_3}{1 + \mu_1\mu_3 H^2/c^2} + \frac{2\mu_3}{1 + 1/_4\psi(\mu)H^2/c^2} + (\mu \to \nu) \right], \quad (14)$$
$$\psi(\mu) = \mu_1\mu_3 + 3\mu_2\mu_3 - 3\mu_4^2.$$

In strong fields

$$\mu_1\mu_3, \ 1/_4\psi(\mu), \ \nu_1\nu_3, \ 1/_4\psi(\nu) \gg c^2 H^{-2},$$
$$\sigma_{11} \sim H^{-2}, \quad \sigma_{12} \sim H^{-1}, \quad \sigma_{13} \sim H^{-3}, \quad \sigma_{22} \sim H^0, \quad \sigma_{23} \sim H^{-2}, \quad \sigma_{33} \sim H^{-2}.$$

Taking into account the difference of the concentrations of the electrons and holes, we have

$$\sigma_{13} = \frac{e\Delta Nc}{H} + e\frac{N}{3}\frac{c^3}{H^3}\left[\frac{1}{\mu_1\mu_3} + \frac{8}{\psi(\mu)} - (\mu \to \nu) \right]. \quad (15)$$

3) $H \parallel C_3 \parallel 3$.

$$\sigma_{11} = \sigma_{22} = eN\left[\frac{1/2(\mu_1 + \mu_2)}{1 + \mu_1\mu_2 H^2/c^2} + \frac{1/2(\nu_1 + \nu_2)}{1 + \nu_1\nu_2 H^2/c^2} \right], \quad (16)$$

$$\sigma_{12} = -\sigma_{21} = eN\frac{H}{c}\left(\frac{\nu_1\nu_2}{1 + \nu_1\nu_2 H^2/c^2} - \frac{\mu_1\mu_2}{1 + \mu_1\mu_2 H^2/c^2} \right) \quad (17)$$

$$\sigma_{33} = eN\left(\mu_3 - \frac{\mu_1\mu_4^2 H^2/c^2}{1 + \mu_1\mu_2 H^2/c^2} + \nu_3 - \frac{\nu_1\nu_4^2 H^2/c^2}{1 + \nu_1\nu_2 H^2/c^2} \right). \quad (18)$$

In strong fields, $\mu_1\mu_2\nu_1\nu_2 \gg c^2 H^{-2}$, $\sigma_{11} \sim H^{-2}$, $\sigma_{12} \sim H^{-3}$, $\sigma_{33} \sim H^0$. With account of the lack of compensation of electrons and holes, we have

$$\sigma_{12} = \frac{e\Delta Nc}{H} + eN\frac{c^3}{H^3}\left(\frac{1}{\mu_1\mu_2} - \frac{1}{\nu_1\nu_2} \right). \quad (19)$$

2. EXPERIMENTAL RESULTS AND THEIR DISCUSSION

The galvanomagnetic effects have been investigated for single crystal samples of SbI ($j \parallel C_1$), SbII ($j \parallel C_2$) and SbIII ($j \parallel C_3$), oriented along the principal crystallographic axes: the bissector C_1, the binary C_2, and the trigonal C_3 (j is the current through the sample).

The orientation of the samples was carried out along cleavage planes with an accuracy to $2°$. The samples were cut from a single monocrystal and submitted to etching in an HF solution with a small addition of HNO_3. The dimensions of the samples were: SbI—$50 \times 3.8 \times 2.8$ mm, Sb III—$50 \times 3 \times 2.4$ mm and SbIII—$28 \times 2.5 \times 2.1$ mm. The measurements were carried out at constant current at temperatures of liquid helium, liquid hydrogen, and liquid nitrogen. The purity of the samples studied could be deduced from the ratio of electric conductivities in the absence of a magnetic field $r_0 = \sigma^0(4.2°K)/\sigma^0(293°K)$, which amounted to 2460 for SbI, 2740 for SbII, and 1810 SbIII.

Figure 1 shows the temperature dependence for the components of the electric conductivity tensor in the absence of a magnetic field, $\sigma^0_{11}, \sigma^0_{22}, \sigma^0_{23}$, measured on the samples SbII, SbI and SbIII, respectively. All the components of the electric conductivity in the range of temperatures 300--1.5°K increase strongly with decrease in the temperature (in the middle part of the interval $\sim T^{-2.5}$), and below 10°K they reveal a tendency toward saturation. Here (as it should be in correspondence with the symmetries of the antimony crystal), $\sigma^0_{11} = \sigma^0_{22}$ over almost the entire temperature range except for helium temperatures, where the scattering of the current carriers by impurities and defects begins to dominate over the acoustical scattering, and
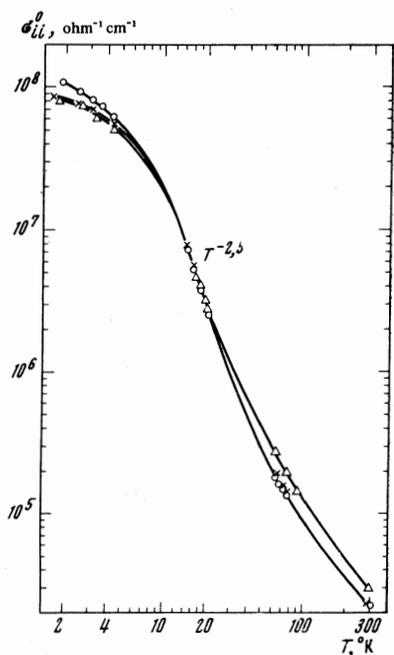
where the individual properties of the samples appear, while the data obtained on the different samples (which differ, for example, in the ratio r_0) become not completely comparable. Thus, for example, in the liquid helium temperature range, the ratio $\sigma^0_{23}/\sigma^0_{11}$, which had a value of 1.3 for 77°K in agreement with the literature data,[8,9] becomes less than unity. For the determination of the true anisotropy of the electric conductivity $\sigma^0_{33}/\sigma^0_{11}$, it is necessary to measure σ^0_{33} and σ^0_{11} on the same specimen. Such measurements on a square sample with dimensions $8.4 \times 8.4 \times 0.4$ cmm and ratio $r_0 = 2690$ showed that upon decrease in the temperature from nitrogen to helium values the anisotropy of the electric conductivity $\sigma^0_{33}/\sigma^0_{11}$ did not really decrease but rose weakly from 1.3 to 1.4.

The temperature dependence of the electric conductivity of antimony, which is shown in Fig. 1, shows that the resistance is determined by the scattering of the carriers by the phonons over a wide temperature range.

Comparison of the temperature dependence of the electric conductivity and the Lorentz number[22] shows that the principal role in the scattering of the carriers in antimony is played by the inelastic scattering mechanisms: in the temperature range from 4 to 10°K—intravalley scattering of the carriers, from 10° to 100°—intervalley scattering. We attempted to describe the temperature dependence of the resistance of antimony by means of the isotropic model, in which account is taken of the contribution made to the resistance by the three components ρ_1, ρ_2 and ρ_3, which correspond respectively to the scattering of the carriers by the impurities and defects and to the acoustic intravalley and intervalley scattering.

Figure 2 shows the experimental temperature dependence of the resistance compared with the value computed on the basis of such a model, which actually assumes the presence of a single group of carriers. The component ρ_1, which corresponds to the residual
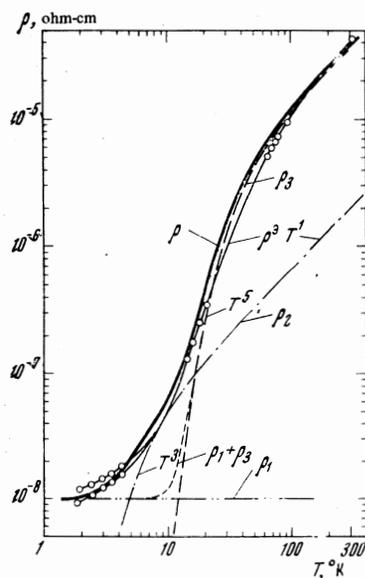

FIG. 1. Temperature dependence of the components of the electric conductivity tensor σ^0_{11} (O), σ^0_{22} (X), σ^0_{33} (Δ), measured on the antimony single crystals SbII, SbI and SbIII, respectively.

FIG. 2. Temperature dependence of the resistance ρ^{exp}—experiment, ρ—total calculated curve ($\rho = \rho_1 + \rho_2 + \rho_3$).

resistance, was estimated from experimental data at helium temperatures, where the curve ρ^{exp} tends toward saturation, $\rho_1 \approx 10^{-8}$ ohm-cm. The component ρ_2 for the intravalley scattering was computed from the Gruneisen-Bloch interpolation formula:

$$\rho_2 = A\tilde{\rho}(\Theta_1)\,(T/\Theta_1)^5$$
$$\times J_5(\Theta_1/T)/J_5(1),$$

where the matching coefficient is A = 0.26; the effective Debye temperature Θ_1 corresponds to double the Fermi momentum and is equal to 25°K in the isotropic approximation;[23] $\tilde{\rho}(\Theta_1)$ is the experimentally determined value of the resistance T = Θ_1 (for tables of the Gruneisen-Bloch function, see, for example,[24]).

The component ρ_3 corresponds, according to our assumption, to the intervalley scattering of the carriers and can be estimated from the formula given in[19]:

$$\rho_3 = B\left/ \operatorname{th}\frac{\hbar\omega_0}{2k_0 T}\left(1 + \frac{1}{2}\operatorname{ch}\frac{\hbar\omega_0}{k_0 T}\right)\right.,$$

where the coefficient B, in addition to the constant that is contained in[19], also takes into account the summation over all valleys of the multi-ellipsoidal model, and ω_0 is the frequency of the phonon which produces the intervalley transition.

According to our estimates,[22] the characteristic Debye temperature for intervalley scattering $\hbar\omega_0/k_0 \approx 100°K$; the coefficient B was chosen to match and is equal to 10^{-4} ohm-cm. It is seen from Fig. 2 that the agreement of the experimental and computed curves is entirely satisfactory; consequently such an analysis, although rather rough, confirms the assumption that an appreciable contribution is made by intervalley scattering to the resistance of antimony at temperatures above 10°K.

The experimental results from the investigation of the magnetoconductivity of antimony at an orientation of the magnetic field along the principal crystallographic directions are shown in Figs. 3—5. The dependences on the magnetic field are also shown in these figures for the various components of the magnetoconductivity tensor at the temperatures 77, 20.4, 14.5, and 4.2°K, computed from the experimentally determined components of the magnetoresistance tensor. The calculation of the components of the tensor from the components of $\hat{\rho}$ is comparatively simple for H ∥ C_2 and H ∥ C_3; in the case H ∥ C_1, the simplifying formulas

$$\sigma_{33} \approx 1/\rho_{33}, \quad \sigma_{11} \approx 1/\rho_{11}, \quad \sigma_{13} \approx \rho_{13}/\rho_{11}\rho_{33},$$

are used. These can be employed in the limiting cases of very strong and very weak magnetic fields if the additional conditions $\rho_{11}\rho_{22} > \rho_{12}^2$, $\rho_{12}\rho_{23} < \rho_{13}\rho_{22}$ are satisfied for the strong fields, and $\Delta\rho_{11} = \rho_{11} - \rho_0 > \rho_{13}^2$, $\Delta\rho_{33} = \rho_{33} - \rho_0 > \rho_{13}^2$ for the weak fields. As estimates show, these conditions were satisfied for helium and hydrogen temperatures when the case of a strong field was important and below 10 kOe for 77°K, when the criteria of a weak field were used.

The experimentally observed dependences of the components of the electric conductivity tensor on the magnetic field are given in Table I. For hydrogen and helium temperatures they are close to the theoretical dependences for the case of strong magnetic fields.
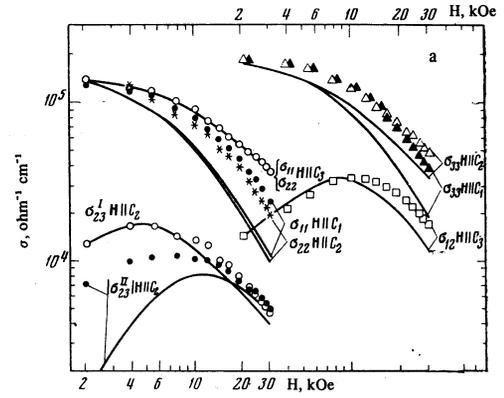

FIG. 3a. Dependence of the components of the electric conductivity tensor on the magnetic field at 77°K. Points—experiment, solid lines—calculation.
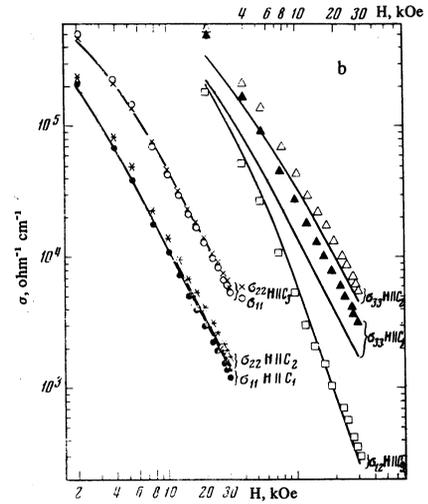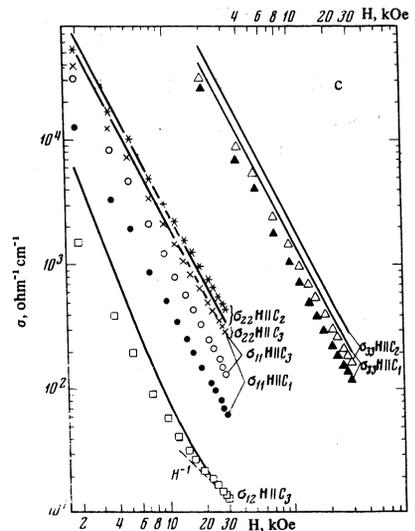

FIG. 3b. The same as in Fig. 3a, but at 20.4°K.

FIG. 3c. The same as in Figs. 3a and 3b, but at 4.2°K.

At helium temperatures in the range of very strong fields (> 20 kOe), the Hall components of the electric conductivity tensor, at the magnetic field orientations H ∥ C_3 (σ_{12}) and H ∥ C_2 (σ_{23}^I), change according to a
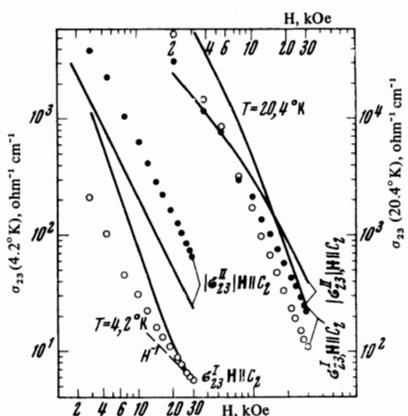
FIG. 4. Dependence of the Hall conductivity σ_{23} ($\mathbf{H} \parallel C_2$) on the magnetic field at temperatures 20.4 and 4.2°K. Points—experiment; solid lines—calculation).
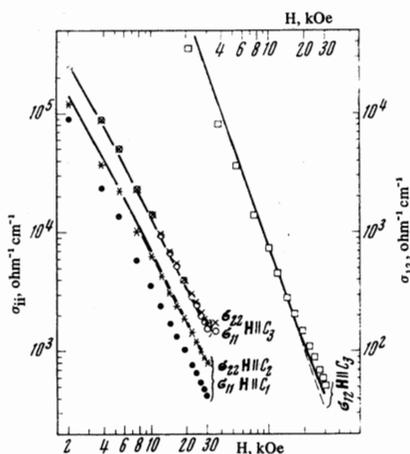

FIG. 5. Dependence of the components of the electric conductivity tensor on the magnetic field for 14.5°K. Points—experiment; solid lines—calculation.

law that is close to H^{-1} ($\sigma_{12} \sim H^{-1.1}$ and $\sigma_{23}^{I} \sim H^{-1.1}$). Such a dependence of the nondiagonal component of the magnetoconductivity tensor indicates incomplete compensation of the contributions of hole and electrons, i.e., violation of the equality of concentrations of electrons and holes. This phenomenon has already been observed previously in pure samples (with a ratio r_0' = $\sigma^0(4.2°K)/\sigma^0(300°K) \approx 3600$) in[12]. From the linear portion of the plot of $\sigma_{12} \sim H^{-1}$ or $\sigma_{23}^{I} \sim H^{-1}$ one can compute the difference in concentrations $\Delta N = p - n$ (in our samples $\Delta N > 0$ always), which turned out to be equal to 5×10^{-4} N for the sample SbI, $\sim 3 \times 10^{-4}$ N for the sample SbII, and $\sim 1 \times 10^{-3}$ N for the sample SbIII ($N = \frac{1}{2}(n + p)$), in qualitative agreement with the change in the ratio of electric conductivities r_0 which characterizes the purity of these three samples. (In[12], the value $\Delta N \approx 2 \times 10^{-3}$ N was found.) A small difference in the concentration of electrons and holes has a very significant effect on the thermomagnetic phenomena in strong magnetic fields, which will be discussed by us in a subsequent article.

In the liquid-nitrogen temperature range, the non-monotonic dependence of the nondiagonal components of the electric conductivity on the magnetic field and the weak change in the diagonal components (the absence of a quadratic fall-off) in fields up to 15—20 kOe indicates the inapplicability of the strong-field approximation. For comparison with theory in this case, one should use the complete formulas (3)—(6), (9)—(14), (16)—(18).

Using data on the dependence of the components of the magnetoconductivity tensor on the magnetic field (and also the values of the components of the electric conductivity tensor without a magnetic field), we have carried out a complete analysis of the experimental results and determined the components of the mobility tensors for electrons and holes at the temperatures 77, 20.3, 14.5, and 4.2°K.

Table I. Dependence on the magnetic field of the components of the electric conductivity tensor for different temperatures and orientations of the magnetic field

T, °K	$\mathbf{H} \parallel C_1$			$\mathbf{H} \parallel C_2$			$\mathbf{H} \parallel C_3$		
	σ_{ij}	Experiment	Theory	σ_{ij}	Experiment	Theory	σ_{ij}	Experiment	Theory
20.4	σ_{11}	$\sim H^{-2}$	H^{-2}	σ_{22}	$H^{-1.9}$	H^{-2}	σ_{11}	$H^{-1.97}$	H^{-2}
	σ_{33}	$\sim H^{-2}$	H^{-2}	σ_{33}	$H^{-1.85}$	H^{-2}	σ_{22}	$H^{-1.97}$	H^{-2}
	—	—	—	σ_{23}^{I}	$H^{-2.5}$	H^{-3}	σ_{12}	$H^{-2.7}$	H^{-3}
	—	—	—	$\vert \sigma_{23}^{II} \vert$	H^{-2}	H^{-2}	—	—	—
14.5	—	—	—	σ_{22}	$H^{-1.9}$	H^{-2}	σ_{11}	$H^{-1.95}$	H^{-2}
	—	—	—	σ_{33}	—	H^{-2}	σ_{22}	$H^{-1.97}$	H^{-2}
	—	—	—	σ_{23}^{I}	$H^{-2.2}$	H^{-3}	σ_{12}	$H^{-2.6}$	H^{-3}
	—	—	—	$\vert \sigma_{23}^{II} \vert$	$H^{-1.9}$	H^{-2}	—	—	—
4.2	σ_{11}	$\sim H^{-2}$	H^{-2}	σ_{22}	$H^{-1.81}$	H^{-2}	σ_{11}	H^{-2}	H^{-2}
	σ_{33}	$\sim H^{-2}$	H^{-2}	σ_{33}	H^{-2}	H^{-2}	σ_{22}	$H^{-1.88}$	H^{-2}
	—	—	—	σ_{23}^{I}*	$H^{-2.8}$	H^{-3}	σ_{12}*	$H^{-2.2}$	H^{-3}
	—	—	—	σ_{23}^{I}**	$H^{-1.1}$	H^{-1}	σ_{12}**	$H^{-1.1}$	H^{-1}
	—	—	—	$\vert \sigma_{23}^{II} \vert$	H^{-2}	H^{-2}	—	—	—

*For H < 10 kOe, when there are no uncompensated holes and electrons.
**For H > 20 kOe, when lack of compensation of electrons and holes in observed.

We have made the following simplifying assumptions:

1. The angles of inclination of the electron and hole ellipsoids were assumed to be known and independent of the temperature. The values used were $\vartheta_c = 6°$ and $\vartheta_h = 26°$, and were obtained from other galvanomagnetic studies[8,9] (the value $\vartheta_h = 26°$ did not agree, generally speaking, with the theoretically calculated value $\vartheta_h = 49°$[1]) and with the value $\vartheta_h = 36°$ obtained from cyclotron resonance,[5] the Shubnikov–de Haas effect[2] and ultrasonic absorption[3], probably owing to the considerable deviation of the shape of the hole cavities of the Fermi surface from ellipsoidal[1]); we took the value obtained from galvanomagnetic data, assuming that suitable allowance has been made for the averaging over the Fermi surface that is characteristic for galvanomagnetic phenomena: the sign of the angle of inclination was taken to be the same as in[8,9,5,1].

2. The number of electrons was assumed to be equal to the number of holes (except for the cases stipulated separately), independent of the temperature and equal to $n = p = N = 4 \times 10^{19}$ cm^{-3} (this is approximately the average value from the data encountered in the literature (see Table 6 in[8] and also[12])).

The first assumption allows us to eliminate the non-diagonal components (relative to the crystal axes) in the mobility tensor, using the formulas

$$\mu_4 = {}^1\!/_2(\mu_2 - \mu_3)\,\mathrm{tg}\,2\vartheta_e, \quad \nu_4 = {}^1\!/_2(\nu_2 - \nu_3)\,\mathrm{tg}\,2\vartheta_h.$$

At hydrogen and helium temperatures, when the condition of a strong magnetic field is satisfied, we can use in the estimates of the components of the mobility the limiting expressions for the galvanomagnetic coefficients, in which additional simplifying approximations are used of the form $\mu_2, \mu_4 \ll \mu_1, \mu_3$; $\nu_2, \nu_4 \ll \nu_1, \nu_3$, and so on; finally, the components of the mobility tensors were matched by means of a high-speed computer so as to fit in the best way the experimental results.

At a temperature 77°K, the condition of a strong magnetic field was not satisfied, and it was necessary to use the general expressions for the galvanomagnetic coefficients. As initial estimates of the components of the mobility tensors of the electrons and holes, we used values averaged from the data of[8,9]; however, subsequent variation of these quantities did not lead to an essential improvement of the agreement between calculation and experiment; therefore just these values were used by us as the experimentally determined values of the mobilities at 77°K.

Finally, the results were converted to the mobilities on the axes of the ellipsoids, in which, by assumption, the mobility tensor is diagonal:

$$\mu_1' = \mu_1, \quad \mu_2' = \frac{1}{2}(\mu_2 + \mu_3) + \frac{1}{2}\frac{\mu_2 - \mu_3}{\cos 2\vartheta_e}, \quad (20)$$
$$\mu_3' = \frac{1}{2}(\mu_2 + \mu_3) - \frac{1}{2}\frac{\mu_2 - \mu_3}{\cos 2\vartheta_e}.$$

The data on the mobilities of electrons and holes for various temperatures are given in Table II.

The accuracy of the determination of the components of the mobility can be estimated at 10–20% (it is estimated by variation of the mobility components when matching the computed data on the magnetoconductivity to experimental with a high-speed computer).

Table II. Components of the mobility tensors along the axes of the ellipsoids for electrons μ_i' and holes ν_i' (in units of 10^4cm^2/V-sec)

T, °K	μ_1'	μ_2'	μ_3'	ν_1'	ν_2'	ν_3'
77 *	1.38	0.032	1.29	2.44	0.186	1.81
20.4	13.5	0.6	6.4	55	8.3	46.3
14.5	30	2.7	10	148	59	115
4.2	75	18	26	1535	440	1120

*Averaged data of Öktü and Saunders [8] and Kechin [9].

In Figs. 3–5, the solid lines show the computed curves obtained by means of the values of the components of the electron and hole mobilities, given in Table II. A comparison of the computer curves with the experiment at 77°K is shown in Fig. 3a. Best agreement is obtained for the most symmetric orientation of the magnetic field H ∥ C$_3$; in the other cases the dependences are given correctly but there are quantitative divergences reaching the values

$$\sigma_{33}^e/\sigma_{33}^{calc} \approx 1.4, \quad \sigma_{22}^e/\sigma_{22}^{calc} \approx 2 \text{ for } H\|C_2,$$
$$\sigma_{11}^e/\sigma_{11}^{calc} \approx 2.3 \qquad\qquad \text{for } H\|C_1.$$

The significant departure of the curve σ_{23}^{II} from experiment (Fig. 3a) for H ∥ C$_2$ in weak magnetic fields is probably explained by failure to take into account the effect of nonequipotential location of the contacts for H = 0.

Best agreement of the computed results with experiment is obtained at a temperature of 20.4°K; the greatest departure is at 4.2°K. This is understandable, since the mobilities were determined from measurements on three samples which have different residual resistance at 4.2°K. At T = 20.4°K, the scattering mechanism was the same for all three samples, i.e., phonons.

This condition is violated somewhat at 14.5°K, which leads to some worsening of the agreement of theory with experiment. Therefore, the coefficient of anisotropy at 4.2°K, determined from measurements on two different samples SbI (SbII) and SbIII, was different from the coefficient of anisotropy determined on the square sample. In the selection of mobility components for the temperature 4.2°K, the true value of the coefficient of anisotropy, measured on the square sample, was taken into account. By virtue of the rather significant divergence in the values of the residual resistance for the samples SbI, SbII and SbIII at 4.2°K, the errors in the determination of the mobilities were extremely large.

As at 77°K, the best agreement of experiment with calculation is obtained at hydrogen temperatures for the case H ∥ C$_3$.

In the calculation of quantities which refer to the temperatures 4.2 and 14.5°K, the weak lack of compensation of the concentration of the electrons and holes was taken into account. The effect of this was discussed above. The uncompensated value ΔN was determined experimentally from the Hall component of the electric conductivity tensor in very strong magnetic fields (where the dependence ~H^{-1} is satisfied). Estimates according to (19) show that in the expression

for σ_{12} ($H \parallel C_3$), the term proportional to H^{-1}, i.e., brought about by the lack of compensation of electrons and holes, begins to dominate over the term $\sim H^{-3}$ in fields exceeding 12 kOe at 4.2°K and at 20.4°K in fields exceeding 140 kOe.

At T = 20.4, the computed values of the magneto-conductivity tensor were determined from the general formulas, since in the given case, for $H < 10$ kOe, the condition of strong field is not satisfied.

From the values of the mobilities, one can compute the anisotropy of the magnetoresistance (see Table III). In this table, our results are compared with the data of[13,25], in which a change was observed in the aniso-tropy of the magnetoresistance of antimony in the tem-perature range from 77 to 4.2°K. Since the asymptote of the transverse magnetoresistance in strong fields is the same for all directions ($\rho \sim H^2$), one can charac-terize the anisotropy of the magnetoresistance by the ratios ρ_{11} ($H \parallel C_1$)/ρ_{11} ($H \parallel C_3$), ρ_{22} ($H \parallel C_2$)/ρ_{22} ($H \parallel C_3$) and ρ_{33}($H \parallel C_1$)/ρ_{33}($H \parallel C_2$).

It is seen from Table III that in the transition from 20.4 to 4.2°K, a significant change takes place in the anisotropy of the magnetoresistance, in accord with the data of[13,25]. However, the explanation of this circum-stance, as is seen from the column "computed" of Table III, can be found not in the change of the energy spectrum, proposed in[13], but in the change of the components of the mobility tensor as a consequence of the replacement of the thermal scattering mechanism by the impurity mechanism.

Bogod, Verkin, and Krasovitskiĭ[25] observed a size effect at helium and hydrogen temperatures, which consists of a dependence of the exponent in the power-law dependence of the resistance on the magnetic field and the anisotropy of the magnetoresistance on the dimensions of the sample. Since the dimensions of our samples were close to those of the "bulk" samples of[25], one can assume that the size effect was not significant in our measurements. Thus, a comparison of the experimental data with those calculated by the formulas of Sec. 1 reveals an agreement with the multi-ellipsoidal model of the energy spectrum for the corresponding relaxation time tensor.

Although the effect of inelasticity of the scattering is less for the electric conductivity than for the
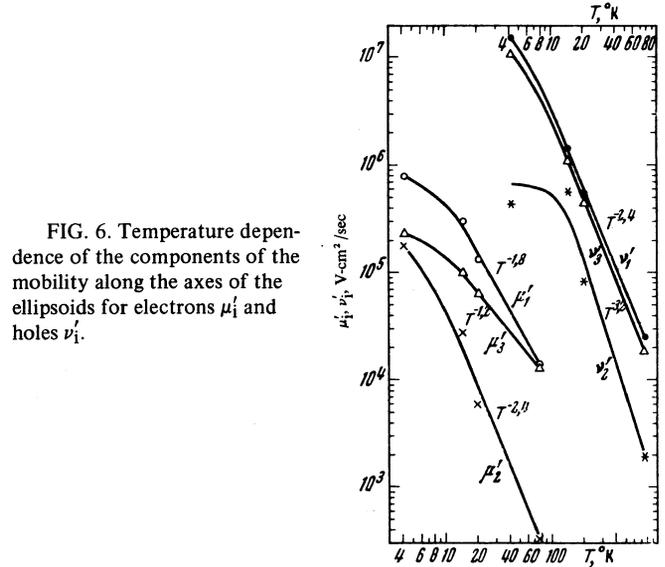

FIG. 6. Temperature depen-dence of the components of the mobility along the axes of the ellipsoids for electrons μ'_i and holes ν'_i.

Lorentz number, an appreciable divergence between experiment and theory can be expected for the mag-netoresistance in this case if the Lorentz number[22] changes by 20—30% because of inelasticity of the type of intervalley scattering. In this way one can explain the rather unsatisfactory agreement between experi-ment and calculation for 77°K, when the effect of in-elasticity, due to intervalley scattering, is maximal.

Figure 6 shows the temperature dependences of the components of the mobility tensor. It is seen that the slope of the temperature dependence is different for the various mobility components, and for the compon-ents μ'_2 and ν'_2 (i.e., for the components along the direction of the elongated electron and hole ellipsoids) the temperature dependence is very strong.

In the case of two scattering mechanisms, we can write for the components of the tensor of the reciprocal relaxation time

$$1/\tau_{\parallel,\perp} = 1/\tau_0 + 1/\tau^i_{\parallel,\perp},$$

where τ_0 is the relaxation time for the intervalley scattering and $\tau^i_{\parallel,\perp}$ are the longitudinal and transverse

Table III. Dependence of the anisotropy of the magnetore-sistance on the temperature under strong magnetic field conditions

T, °K	ρ_{11}(H ∥ C_1)/ρ_{11}(H ∥ C_3)			ρ_{22}(H ∥ C_2)/ρ_{22}(H ∥ C_3)				ρ_{33}(H ∥ C_1)/ρ_{33}(H ∥ C_2)		
	Our data	Data of [13] *	Com-puted	Our data	Data of [13] *	Data of [25] **	Com-puted	Our data	Data of [13] *	Com-puted
77***	2	0.8	3.6	2.2	3.2		4.1	**1.3**	**1.25**	1.8
20.4	4.8	1.95	4.3	3.4	2.3	4	4.3	1.8	1.75	2.7
14.5	4		1.9	2.1		3	1.9	1.9		1.8
4.2	2.3	0.9	1	0.7	0.8	1,5	0.9	1,4	1.35	1.3

*Sample with ratio r'_0 = 730 and dimensions 1 X 1 X 10 mm.

**Sample with ratio r'_0 = 1650 and dimensions 4 X 4 X 25 mm.

***For 77°K, the anisotropy of the magnetoresistance was measured in a field H = 30 kOe, when the strong magnetic field condition was no longer satisfied. Calculation of the anisotropy of the magnetoresistance for 77°K was also satisfied for H = 30 kOe.

components of the relaxation time tensor for intravalley scattering (here we shall approximate the carrier ellipsoids in antimony by ellipsoids of revolution).

In the Herring approximation,[2] the relaxation time for intervalley scattering can be regarded as isotropic If we assume that $\tau_{\parallel}^i > \tau_{\perp}^i$, then the contribution of intervalley scattering turns out to be more substantial in the longitudinal case than in the transverse, which leads to an increase in the exponent of the temperature dependence of the corresponding component of the mobility.

The temperature dependence of the electron mobility $\mu_3' \sim T^{-1.2}$ is close to the theoretical value without account of intervalley scattering (T^{-1}), which permits us to estimate the constant $\mathscr{E}_1$ of the deformation potential from the formula (see[15])

$$\mu_3' = \frac{2^{1/2}\pi^{1/2}e\rho v^2}{3m_3^*(m_1^*m_2^*m_3^*)^{1/2}k_0 T\zeta^{1/2}\mathscr{E}_1^{1/2}} \tag{21}$$

where e is the electronic charge, ρ the mass density (for antimony, $\rho = 6.7$ g/cm^3), v the speed of sound; $\zeta = \hbar^2(3\pi^2 N)^{2/3}/2m_d^*$ is the chemical potential of the electrons, m_d^* the mass density of states. The estimate (with use of the isotropic value for the sound speed v = 2.5×10^5 cm/sec[23]) gives $\mathscr{E}_1 = 6$ eV, which is approximately three times larger than the value of $\mathscr{E}_1$ computed from the lattice thermal conductivity in[23].

In conclusion, the authors express their gratitude to S. S. Shalyt for his initiative conducting the present investigation and useful advice, to I. Ya. Korenblit for valuable remarks and fruitful discussion of the results, and V. V. Mikhaĭlov for help in the programming for the highspeed computer.

[1] L. M. Falicov and P. J. Lin, Phys. Rev. 141, 562 (1966).

[2] J. Ketterson and Y. Eckstein, Phys. Rev. 132, 1885 (1963).

[3] L. Erickson, O. Beckman, and S. Hörnfeldt, J. Phys. Chem. Solids 25, 1339 (1964).

[4] L. R. Windmiller and M. G. Priestley, Solid State Com. 3, 199 (1965).

[5] W. R. Datars and J. Vanderkooy, IBM J. Res. Dev. 8, 247 (1964).

[6] L. R. Windmiller, Phys. Rev. 149, 472 (1966).

[7] N. B. Brandt, N. Ya. Minina, and Chu Chen-kang, Zh. Eksp. Teor. Fiz. 51, 108 (1966) [Soviet Phys.-JETP 24, 73 (1967)].

[8] O. Oktu and G. A. Saunders, Proc. Phys. Soc. (London) 91, 156 (1967).

[9] V. V. Kechin, Fiz. Tverd. Tela 9, 3595 (1957) [Soviet Phys.-Solid State 9, 2680 (1968)].

[10] M. C. Steele, Phys. Rev. 99, 1751 (1955).

[11] G. N. Rao, N. H. Zebouni, C. G. Grenier, and J. M. Reynolds, Phys. Rev. 133, A141 (1964).

[12] J. B. Long, C. G. Grenier, and J. M. Reynolds, Phys. Rev. 140, 187 (1965).

[13] Yu. A. Bogod, V. V. Eremenko, Zh. Eksp. Teor. Fiz. 53, 473 (1967) [Soviet Phys.-JETP 26, 311 (1968)].

[14] N. B. Brandt, E. A. Svistovaand, and T. V. Gorskaya, Zh. Eksp. Teor. Fiz. 53, 1274 (1967) [Soviet Phys.-JETP 26, 745 (1968)].

[15] C. Herring and E. Vogt, Phys. Rev. 101, 944 (1956).

[16] A. G. Samoĭlovich, I. Ya. Korenblit, I. V. Dakhovskiĭ, and V. D. Iskra, Fiz. Tverd. Tel. 3, 2939 (1961) [Soviet Phys-Solid State 3, 2148 (1962)].

[17] B. A. Efimova, I. Ya. Korenblit, V. I. Novikov, and A. G. Ostroumov, Fiz. Tverd. Tela 3, 2747 (1961) [Soviet Phys.-Solid State 3, 2004 (1962)].

[18] T. C. Harman, J. M. Honig and B. M. Tarmy, Adv. Energy Conversion 5, 1 (1965).

[19] I. Ya. Korenblit, M. E. Kuznetsov, V. M. Muzhdaba, and S. S. Shalyt, Zh. Eksp. Teor. Fiz. 57, 1867 (1969) [Soviet Phys.-JETP 30, 1009 (1970)].

[20] M. I. Kaganov and V. G. Peschanskiĭ, Zh. Eksp. Teor. Fiz. 35, 1052 (1958) [Soviet Phys.-JETP 8, 734 (1959)].

[21] N. E. Alekseevskiĭ, N. B. Brandt, and T. I. Kostina, Dokl. Akad. Nauk SSSR 105, 46 (1955).

[22] N. A. Red'ko, M. S. Bresler, and S. S. Shalyt, Fiz. Tverd. Tela 11, 3005 (1969) [Soviet Phys.-Solid State 11, 2435 (1970)].

[23] R. S. Blewer, N. H. Zebouni, and C. G. Grenier, Phys. Rev. 174, 700 (1968).

[24] G. K. White, Experimental Techniques in Low Temperature Physics (Russian Translation, Fizmatgiz, p. 356).

[25] Yu. A. Bogod, B. I. Verkin, and V. B. Krasovsitskiĭ, ZhETF Pis. Red. 12, 224 (1970) [JETP Lett. 12, 155 (1970)].

[26] C. Herring, Bell Syst. Tech. J. 34, 237 (1955).

Translated by R. T. Beyer
29